（様式５）(Style5)

学位論文全文に代わる要約
Extended Summary in Lieu of Dissertation

氏名：　Sirinapa Chungopast
Name

学位論文題目：
Title of Dissertation

Functional analysis of nodule senescence in *Lotus japonicus* inoculated with *Mesorhizobium loti*.
（ミヤコグサ根粒菌感染による根粒老化の機能解析）

学位論文要約：
Dissertation Summary

Senescence process was considered important for development life cycle of the legumes and influencing the agricultural. A representative study of symbiosis as *Mesorhizobium loti* with *Lotus japonicus* under the conditions nodule senescence stage was verified. Besides *M. loti* glutamine synthetase I (GS I)-deficiency mutant (STM30) also tells us about a possible way of outset senescence. We checked the phenotype and chemical characteristics in the STM30 mutant-infected nodule, illustrated early senescent nodule. The small size and green nodule appeared with the STM30 mutant-infected nodule (Figure 1). We found that the main characteristics changes in nodules senescence is the irreversible loss of nitrogen fixing ability. It was significantly decreasing 66 % and 47.6 % at late stage of wild type (WT)- and STM30 the mutant- infected nodule respectively, compared with initial stage. Western blot analysis showed that leghemoglobin protein was slightly lower in the STM30 infected nodule at 9 wpi. Membrane damage can be seen in cross section through an optical microscope. The leaves turn into yellowish described by reduction of chlorophyll concentration around 35% at 7wpi. Defect of GSI in bacteroid was possible reasons that cause premature aging in *L. japonicus* due to a numerous green nodules, small nodule size, and 40 % acetylene reduction (Figure 2) activity decreasing as well as low amount of glutamic acid and glutamine content (Figure 3) and high carbon-to-nitrogen ratio (CN ratio) in Table 1. The CN ratio are an indicator for nitrogen limitation, which is effect on the plants growth and development. Althoung the percentage of carbon was stable but the percentage of nitrogen in the STM30-infected nodule is very low. The glutamine synthetase and glutamate synthase activities in the nodules were decrease 12.3 % and 42.31 %, respectively in *L. japonicus* nodules (Figure 3a and b). This result probably effected on protein level and enzyme activity including led to senesce in leaves. Regarding a gene expression, the high expression of cysteine protease

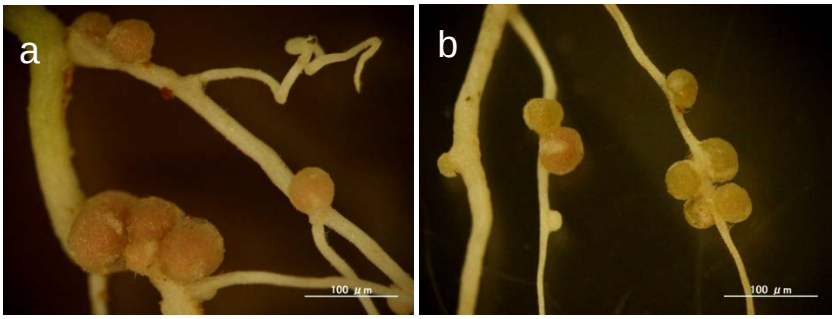

Figure 1 Phenotype of nodules. The color of the nodules inoculated with the wild-type *M. loti* (a, pink nodule) and STM30 (b, pink and green small nodules) at four weeks post-inoculation were determined. Bar = 100μm.

gene was observed at 4 and 7 wpi (Figure 5). The cysteine protease gene expression normally appears to be paralleled with programmed cell death events. However, the STM30-infected nodule showed early expressed at 4 wpi that contributed to early senescent nodule.

It is remarkable that a higher concentration of nitric oxide (NO) per nodule was accumulated in the STM30 inoculated nodule (Table 2). NO signaling inducts of cell death, defense genes and can interact with reactive oxygen species (ROS). In Figure 6, the high ratio of dead bacteroid per living bacteroid cell was presented in the STM30-infected nodules. It also clearly found dead bacteroid cell from Figure 7. These results indicate that GS deficiency in *M. loti* induces early nodule senescence in *L. japonicus*.

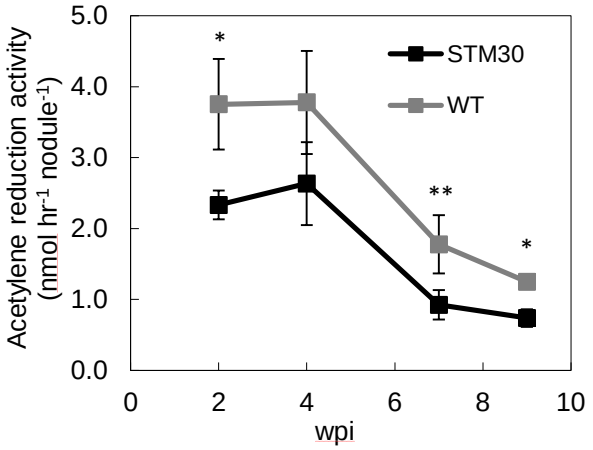

Figure 2 Acetylene reduction activity of *L. japonicus* inoculated with WT and the STM30 mutant during nodule development. All data are shown ± SD. Statistically significant differences compared with the WT-infected nodules are indicated with * (P<0.05), ** (P<0.01).

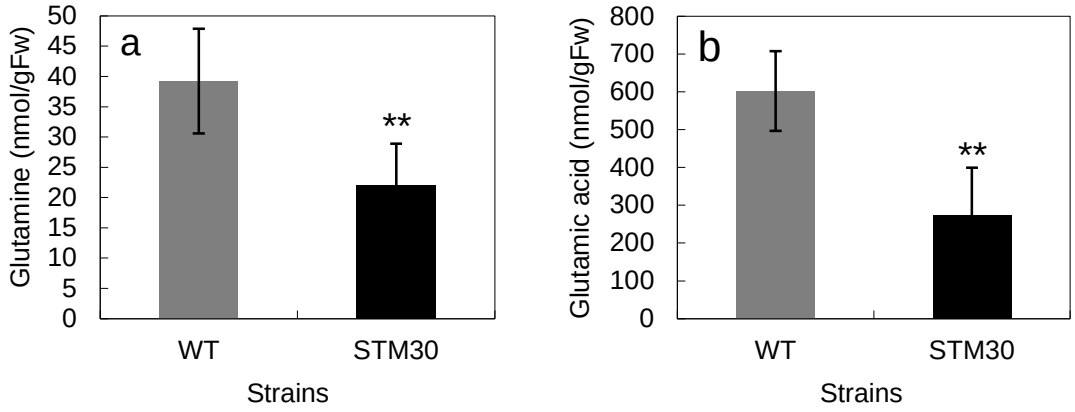

Figure 3 The glutamine (a) and glutamic acid (b) concentration in the WT- and the STM30-infected nodule at 7 wpi were measured by amino-acid analyzer. All data are shown ± SD. Statistically significant differences compared with the WT-infected nodules are indicated with ** (P<0.01).

Table 1 The percentage of carbon, nitrogen, and the ratio of carbon to nitrogen in leaves and the WT- and the STM30 infected nodules.

Tissues	Wpi	Wild-type			STM30		
		C%	N%	C/N ratio	C%	N%	C/N ratio
Leaves	2	41.05±1.60	2.92±0.08	14.05±0.54	41.35±0.18	2.08±0.09**	19.91±0.84**
	4	42.65±0.90	4.09±0.07	10.44±0.15	42.70±0.66	3.23±0.18**	13.25±0.74**
	7	45.65±1.04	4.25±0.15	10.74±0.30	45.89±1.05	3.51±0.07**	13.06±0.26**
Nodules	2	42.23±0.91	6.66±0.40	6.35±0.34	41.97±1.05	5.32±0.23**	7.90±0.24**
	4	44.84±1.12	8.18±0.44	5.49±0.19	43.29±0.49*	6.01±0.19**	7.21±0.27**
	7	45.86±2.46	8.38±0.63	5.49±0.38	45.91±1.08	5.77±0.42**	8.00±0.71**

Values are the mean ± standard deviations (n = 9). Statistical significant differences compared with WT-infected nodule are indicated with **(P<0.01). Wpi, weeks post inoculation

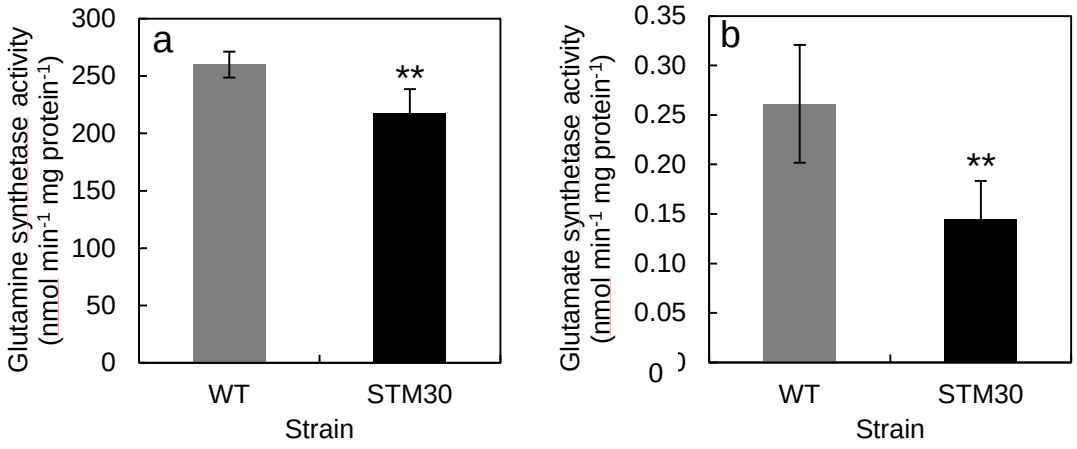

Figure 4 Specific activities of glutamine synthetase: GS (a) and glutamate synthase: GOGAT (b) in nodule of wild-type *M. loti* (WT) and STM30 infection at 4wpi. The GS activity was measured by colorimetric method. All data are shown ± SD. Statistically significant differences compared with the wild-type-inoculated nodules are indicated with ** (*P*<0.01).

Table 2 Concentration of Nitric oxide in nodules of *L. japonicus* inoculated with WT or STM30 mutant. Values are the mean ± standard deviations and the significant difference test was indicated ***P* < 0.01

Wpi	RFU/min/nodule	
	WT	STM30
4	1.5 ± 0.2	1.9 ± 0.1**
7	8.8 ± 0.8**	8.0 ± 0.7

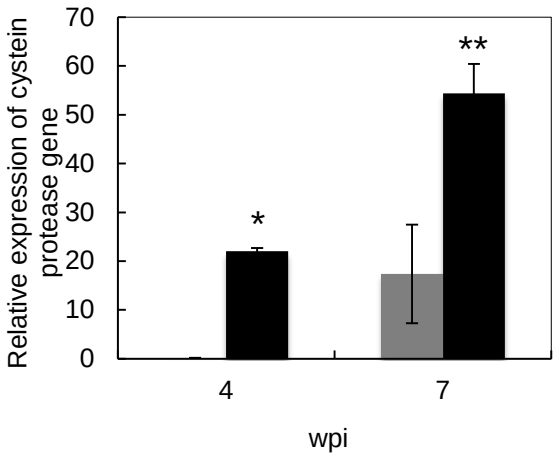

Figure 5 The cysteine protease gene expressed in the nodules inoculated with STM30 (■) or wild-type (■) *M. loti*. The qRT-PCR was performed using the cDNA of nodules harvested at 4 and 7 weeks post-inoculation. Ubiquitin is a reference gene. All data are shown ± SD. Statistically significant differences compared with wild-type nodule are indicated with * (P<0.05), **(P<0.01).

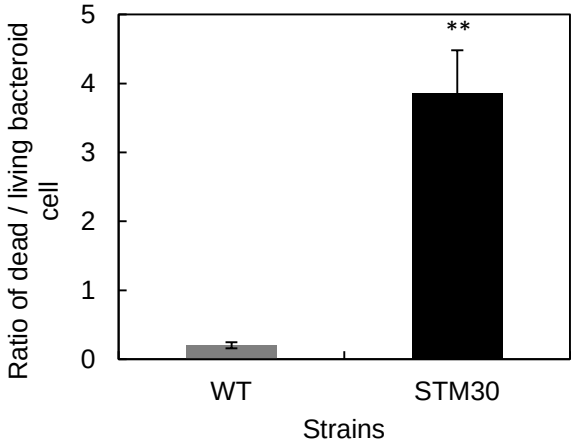

Figure 6 Ratio of dead bacteroid per living bacteroid cell in the nodule. The ratio was high in the mutant-infected nodule at 4 weeks post inoculation. Data are shown ± SD. Statistically significant differences compared with the WT-infected nodules are indicated with ** (P<0.01).

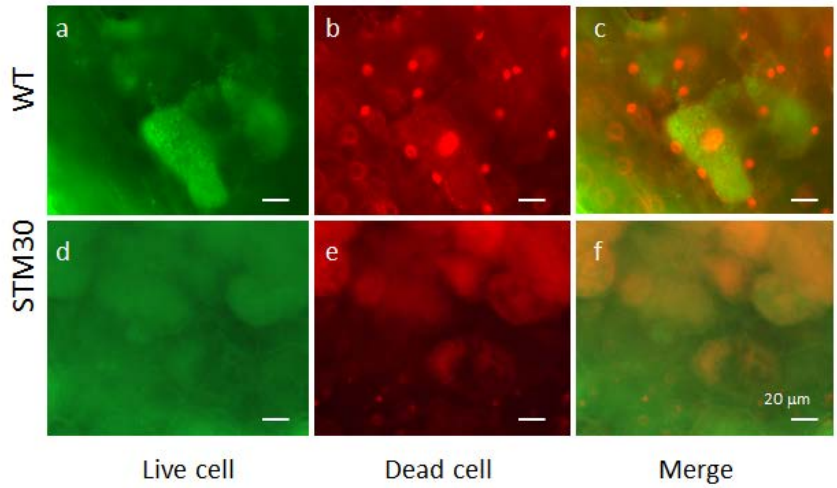

Figure 7 Live (a, d) and dead (b, e) bacteroid cell, and merge image (c, f) of the WT- and the STM30-infected nodules at 4 wpi. The nodules section thick = 50-70 µm and bar = 20 µm.

The senescence is a highly complex process and control by genetic. *Lotus japonicus* is determinated nodule that forms senescence from central of the nodules. To achieve a greater understanding of regulated-genes in transcription level thus microarray was examined in senescent nodule. The Agilent 4×44 microarray chip was designed for *Lotus* nodule transcript sequences. The nodule at 2, 4 and 8 weeks post inoculation (wpi) were analyzed. Result of molecular technique precisely exhibited transcriptomic changed of infected-nodule senescence both up-and down-regulations as compared with 2wpi and 8wpi. After filtered out data which were less than 10% coefficient of variation using the information in the more than 2-fold, and less than 0.5-fold, the microarray data showed 641 up-regulated genes and 416 down-regulated genes among total 20,165 genes during nodule senescence. There were divided distinct profile pattern into four clusters (Figure 8). We emphasized cluster 1 and 2 (Figure 9) because they showed up-regulation at nodule senescence. Mostly genes linked stress response, redox homeostasis, hormone metabolism, and membrane transport. A senescence marker, cysteine protease gene (*cyc*), was up-regulation at 8 wpi. In contrast, down-regulation of genes (Figure 9) related defence mechanism. RT-PCR using 72 specific primers as well proved for confirming gene expression results obtained from microarray analysis.

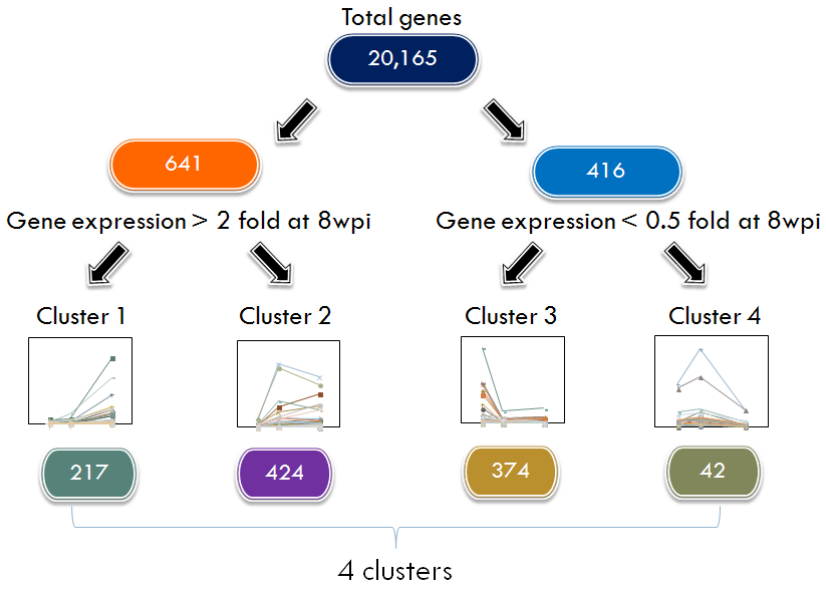

Figure 8 Diagram of screening and gene clustering relevant to nodule senescence filtering percentage of coefficient of variation.

（様式５）(Style5)

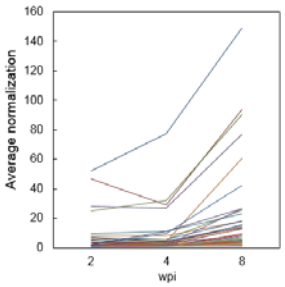

Cluster 1 (217)

ID number	Annotation	2 Wpi Average normalized	2 Wpi SD normalized	2 Wpi %CV	4 Wpi Average normalized	4 Wpi SD normalized	4 Wpi %CV	8 Wpi Average normalized	8 Wpi SD normalized	8 Wpi %CV
chr2.CM0191.580.r2.m	Nij21 [Lotus japonicus]	52.30	5.42	10.36	77.67	16.04	20.64	148.91	14.81	9.95
chr1.CM0012.2130.r2.m	tonoplast intrinsic protein	46.64	1.88	4.03	28.84	0.74	2.56	93.89	2.64	2.81
chr5.CM0456.170.r2.d	acidic chitinase	27.98	2.53	9.04	27.09	4.31	15.91	76.86	7.26	9.45
LjSGA_096088.1	pathogenesis-related protein PR10	24.91	2.36	9.48	32.13	1.73	5.39	90.15	6.29	6.98
LjSGA_043683.1	U-box domain-containing protein 20-like	9.80	0.33	3.38	11.51	0.25	2.17	23.09	0.18	0.78
chr5.CM0071.800.r2.m	CBL-interacting protein kinase 4	8.50	0.79	9.34	8.42	0.07	0.82	17.99	1.25	6.93
LjSGA_025506.1	bon1-associated protein 2-like	7.17	0.81	11.27	5.94	0.37	6.25	18.25	1.43	7.83
chr2.CM0608.1150.r2.m	uncharacterized protein	6.86	0.40	5.85	4.38	0.43	9.77	15.33	0.93	6.08
LjSGA_057224.1	trypsin inhibitor	6.01	0.19	3.14	5.67	0.50	8.87	25.85	1.45	5.62
chr1.CM0433.130.r2.d	BURP domain-containing protein	5.21	0.36	7.00	2.04	0.38	18.69	13.03	0.51	3.87
chr1.LjT14M06.150.r2.d	uncharacterized protein	5.08	0.16	3.11	4.64	0.11	2.35	13.66	0.41	3.00
chr3.LjT36L22.160.r2.a	nicotianamine synthase	3.82	0.37	9.73	4.40	0.65	14.84	60.67	5.33	8.78
chr3.CM0213.540.r2.m	ATP-binding casssette	3.41	0.04	1.16	3.86	0.24	6.16	6.83	0.31	4.53
chr4.CM0432.2980.r2.d	S-adenosyl-L-methionine: 2,7,4-trihydroxyisoflavanone 4 - O-methyltransferase	3.19	0.10	3.00	2.93	0.01	0.22	8.83	0.12	1.32
chr1.CM0320.110.r2.d	probable wrky transcription factor 70-like	2.57	0.06	2.27	1.96	0.01	0.51	6.76	0.17	2.51
chr2.CM0610.140.r2.m	ethylene-responsive transcriptional coactivator-like protein	2.35	0.87	37.03	11.41	4.06	35.57	26.40	9.51	36.04
chr4.CM0026.1220.r2.a	cytochrome P450	2.29	0.04	1.61	2.66	0.19	7.00	15.81	1.00	6.35
chr5.CM0180.30.r2.d	aspartic proteinase nepenthesin-1-like	2.19	0.09	4.08	2.52	0.03	1.00	5.16	0.18	3.55
LjSGA_059392.1	kunitz-type trypsin inhibitor-like 2 protein	2.18	0.03	1.21	9.57	0.85	8.89	42.65	1.61	3.77
chr2.CM0249.1390.r2.m	isoflavone reductase	2.15	0.16	7.44	3.86	0.46	11.84	14.02	0.29	2.04

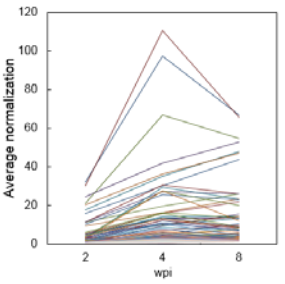

Cluster 2 (424)

ID number	Annotation	2 Wpi Average normalized	2 Wpi SD normalized	2 Wpi %CV	4 Wpi Average normalized	4 Wpi SD normalized	4 Wpi %CV	8 Wpi Average normalized	8 Wpi SD normalized	8 Wpi %CV
chr1.CM0195.250.r2.m	cysteine proteinase 15A-like	32.06	1.32	4.12	97.33	2.52	2.59	66.84	2.98	4.45
chr1.CM0295.970.r2.m	peptide transporter PTR3-a	30.02	3.19	10.63	110.70	8.46	7.64	65.69	5.05	7.69
chr2.CM0065.600.r2.d	uncharacterized protein	21.03	0.03	0.14	66.63	0.77	1.16	54.48	1.05	1.93
chr3.CM0135.890.r2.a	cyclophilin	24.45	1.17	4.80	41.99	0.19	0.46	52.82	1.25	2.37
LjSGA_015484.1	cysteine protease	17.53	0.63	3.59	34.97	0.85	2.44	47.98	1.24	2.59
chr4.CM0126.510.r2.m	subtilisin-like protease SDD1-like	20.26	0.90	4.46	36.20	3.61	9.98	47.11	2.20	4.66
LjSGA_062791.1	no hit	15.81	1.52	9.64	30.23	1.53	5.05	43.71	2.98	6.83
chr1.CM2079.120.r2.a	UNC93-like protein	11.24	0.66	5.88	30.39	1.73	5.70	25.93	1.66	6.39
chr1.CM0017.470.r2.a	transaldolase	11.31	1.22	10.74	19.46	2.52	12.93	25.81	2.44	9.44
LjT42E21.90.r2.m	wound-induced protein	11.07	0.61	5.48	26.92	1.85	6.87	25.75	1.17	4.54
chr4.CM0432.790.r2.m	carboxypeptidase C	2.88	0.04	1.33	29.32	1.49	5.07	23.29	0.42	1.80
LjSGA_051679.1	cysteine synthase	9.10	0.16	1.74	16.16	0.49	3.04	23.16	0.12	0.51
chr4.LjT13G24.170.r2.a	cytochrome p450 like TBP	9.95	0.12	1.18	25.66	0.95	3.71	23.02	0.52	2.24
LjSGA_019294.2	type 2 metallothionein	5.13	0.10	2.00	15.76	0.06	0.38	21.90	0.38	1.74
chr1.CM0591.60.r2.m	no hit	3.76	0.03	0.85	27.61	0.50	1.80	19.77	0.57	2.87
LjSGA_142964.1	nodulin-like protein	0.73	0.07	10.03	9.15	0.51	5.55	15.28	1.14	7.44
chr4.CM0165.230.r2.d	calmodulin-like protein	4.40	0.19	4.40	14.11	0.66	4.69	14.07	0.43	3.03
chr4.CM0075.30.r2.m	uncharacterized protein	5.52	0.29	5.27	9.90	0.29	2.93	14.04	0.83	5.95
chr3.CM0160.370.r2.m	uncharacterized protein	5.10	0.06	1.19	13.33	0.25	1.91	13.48	0.54	4.04
chr3.CM0160.350.r2.m	proline-rich protein	5.27	0.16	3.12	13.02	0.14	1.09	13.35	0.58	4.36

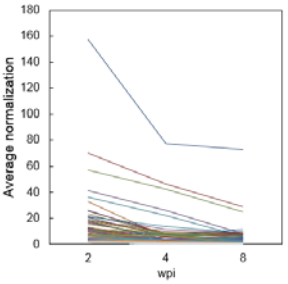

Cluster 3 (374)

ID number	Annotation	2 Wpi Average normalized	2 Wpi SD normalized	2 Wpi %CV	4 Wpi Average normalized	4 Wpi SD normalized	4 Wpi %CV	8 Wpi Average normalized	8 Wpi SD normalized	8 Wpi %CV
chr1.CM0104.2620.r2.m	arabinogalactan peptide 14	157.19	6.16	3.92	77.18	0.20	0.26	73.07	3.94	5.39
chr1.CM0125.390.r2.m	probable peptide nitrate transporter at2g40460-like	70.29	2.57	3.66	46.27	3.04	6.58	28.98	1.30	4.49
chr4.CM0337.580.r2.m	EKN protein	57.04	5.60	9.81	42.54	3.05	7.16	24.94	1.50	6.01
chr4.CM0227.40.r2.d	AP2 erf domain-containing transcription factor	41.62	2.69	6.46	25.98	0.20	0.76	7.87	0.24	3.00
chr1.CM0644.890.r2.m	cu zn superoxide dismutase	36.45	2.04	5.60	21.99	3.06	13.93	5.77	1.08	18.70
chr3.CM0282.1000.r2.m	early nodulin-like protein 2-like	32.96	2.06	6.26	5.06	0.33	6.44	7.62	0.45	5.87
chr4.CM0042.2230.r2.m	calmodulin 24-like protein	26.36	0.46	1.73	6.84	0.34	4.98	11.61	0.16	1.39
chr5.CM1077.360.r2.a	glutamine expressed	25.35	1.12	4.40	8.07	0.31	3.82	8.53	0.20	2.34
chr1.CM0104.2710.r2.a	uncharacterized protein loc100798848 isoform 1	23.50	1.02	4.33	7.39	0.16	2.19	7.91	0.16	1.96
chr2.CM0021.560.r2.m	uncharacterized protein	21.61	0.02	0.08	11.69	0.54	4.61	8.98	0.16	1.76
chr4.CM0046.1620.r2.m	aquaporin NIP1-2	21.09	1.97	9.34	13.69	1.76	12.78	8.84	0.98	11.13
chr1.CM0017.1450.r2.d	farnesylated protein	20.63	1.86	8.99	5.80	0.55	9.49	8.62	0.86	10.02
chr1.CM0398.350.r2.d	dehydration-induced protein ERD15	20.51	0.94	4.58	6.42	0.08	1.23	9.97	0.44	4.42
chr4.CM0006.210.r2.d	no hit	18.99	1.16	6.09	9.66	0.01	0.11	8.25	0.18	2.22
chr3.CM0590.380.r2.d	uncharacterized protein	18.42	1.48	8.01	8.50	0.46	5.37	7.54	0.75	9.89
chr2.CM0608.1430.r2.m	uncharacterized protein	17.86	0.44	2.47	3.49	0.31	8.87	6.70	0.54	8.04
chr3.CM1570.70.r2.a	IAA-amino acid hydrolase ILR1-like protein	17.51	0.49	2.79	2.84	0.96	33.83	3.48	1.29	37.05
LjSGA_023779.1	copoporphyrinogen III oxidase	17.47	1.47	8.42	7.98	0.26	3.25	6.15	0.57	9.27
chr2.CM0903.320.r2.a	uncharacterized protein loc100815940	16.71	0.16	0.96	5.63	0.14	2.42	7.28	0.02	0.31
chr1.LjT04N09.160.r2.d	NAC domain protein	16.50	0.12	0.73	5.31	0.09	1.66	7.91	0.10	1.21

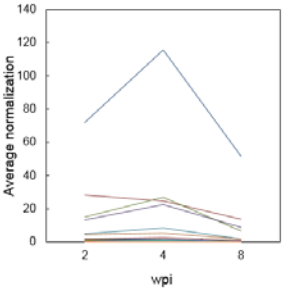

Cluster 4 (42)

ID number	Annotation	2 Wpi Average normalized	2 Wpi SD normalized	2 Wpi %CV	4 Wpi Average normalized	4 Wpi SD normalized	4 Wpi %CV	8 Wpi Average normalized	8 Wpi SD normalized	8 Wpi %CV
chr4.CM0337.590.r2.m	vacuolar iron transporter homolog 4-like	72.10	6.53	9.06	115.67	11.23	9.70	51.63	2.09	4.05
chr6.CM1514.140.r2.m	dihydroneopterin aldolase	28.40	2.48	8.72	24.97	3.69	14.78	13.89	3.40	24.49
LjT36K06.70.r2.d	sugar transporter sweet1-like	15.06	4.14	27.51	26.85	7.31	27.23	6.78	1.72	25.32
chr4.CM0414.440.r2.d	metal transporter	13.43	2.25	16.79	22.61	5.03	22.24	8.84	1.94	22.01
chr5.LjT43D06.110.r2.d	vegetative lectin	4.79	0.23	4.80	8.58	0.00	0.03	1.80	0.10	5.27
chr2.CM0021.1330.r2.m	expansin-like B1-like	4.26	0.34	7.96	5.54	0.50	9.01	1.90	0.13	7.06
chr1.CM1868.110.r2.a	ubiquitin system component CUE protein	1.67	0.01	0.87	1.97	0.06	3.25	0.55	0.03	4.65
LjSGA_060891.2	inositol phosphate kinase	1.66	0.12	7.18	2.77	0.35	12.61	0.91	0.07	7.67
chr4.CM0307.380.r2.d	mitochondrial substrate carrier family protein	1.35	0.02	1.26	1.47	0.03	2.26	0.67	0.01	2.02
chr1.CM0012.190.r2.m	probable membrane-associated kinase regulator 4-like	1.15	0.02	1.74	1.11	0.04	3.66	0.49	0.01	1.03
chr2.CM0081.530.r2.d	quinone oxidoreductase-like protein	0.92	0.05	5.22	0.93	0.04	4.73	0.31	0.02	5.09
LjSGA_016572.1	ethylene-responsive transcription factor ERF118	0.82	0.04	5.34	0.84	0.05	5.97	0.40	0.00	0.03
chr1.CM0109.110.r2.d	uncharacterized protein	0.80	0.05	6.54	1.01	0.08	7.53	0.36	0.04	11.35
LjSGA_047220.1	zinc finger protein constans-like 9	0.77	0.04	4.66	0.67	0.03	4.92	0.24	0.01	3.38
LjSGA_039721.1	glucose 1-dehydrogenase-like	0.75	0.02	3.10	1.04	0.04	3.79	0.31	0.02	6.31
chr2.CM0373.110.r2.d	phospholipase a2	0.65	0.03	4.54	0.57	0.03	5.22	0.33	0.00	0.67
chr5.CM0657.290.r2.m	cytosolic Fe-S cluster assembly factor nbp35	0.63	0.06	8.79	0.82	0.12	14.39	0.22	0.03	11.66
LjSGA_084433.1	expansin B3	0.63	0.05	7.61	0.50	0.00	0.01	0.16	0.00	1.82
LjSGA_087846.1	peptide chain release factor 2	0.61	0.01	1.31	0.69	0.02	3.38	0.24	0.01	2.78
chr6.CM0013.1230.r2.m	uncharacterized protein	0.57	0.00	0.16	0.71	0.03	4.81	0.17	0.01	4.36

Figure 9 Expression profiles of clusters 1-4 during nodule senescence. The total number of genes in each cluster is indicated in parentheses. The data are expressed as the average normalization, the standard deviation (SD), and the coefficient of variation (CV). The top twenty genes in clusters 1-4 according to the expression pattern of 2, 4, and 8 wpi are shown, respectively.

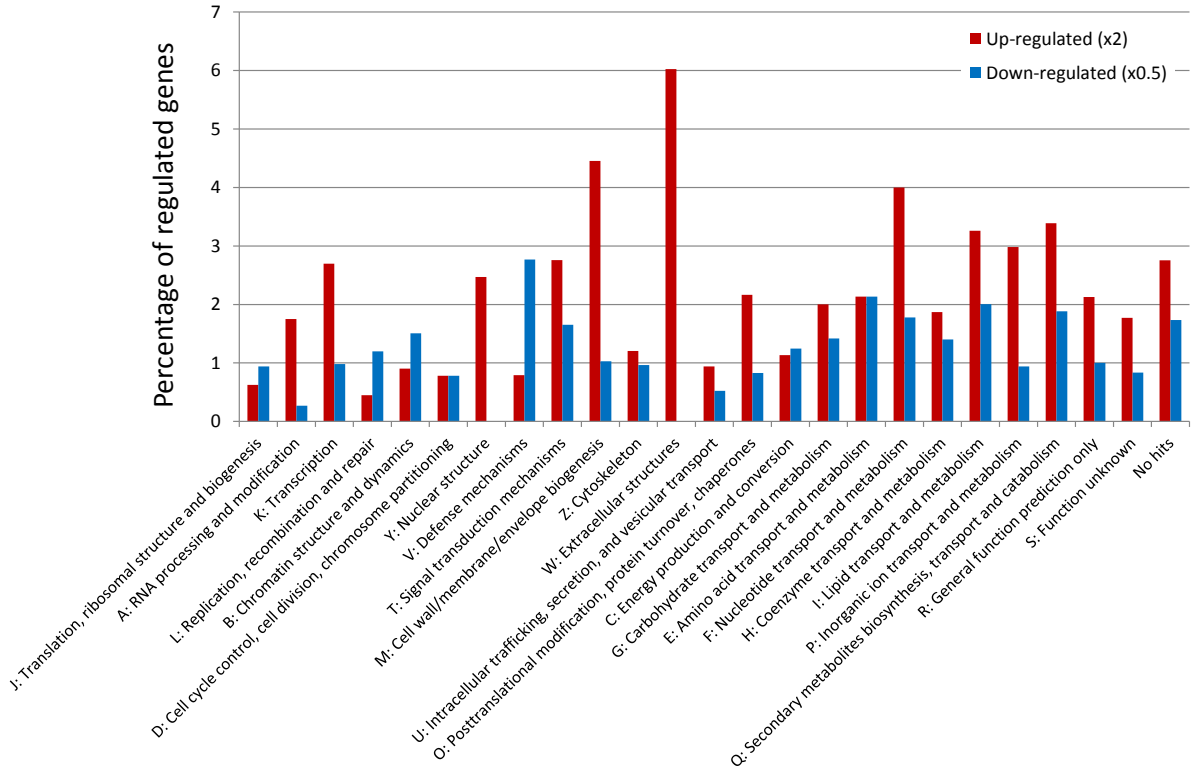

Figure 10 Gene ontology (GO) were used to classify the functions of the predicted senescence-associated genes using eukaryotic orthologous groups (KOG) database.

Gene ontology (GO) indicated function of genes most relevant to metabolism, and cellular processes and signaling at late stage by eukaryotic orthologous groups (KOG) database of proteins domain (Figure 10). They suggested that a number of significantly up-regulated genes at 8wpi related to cell wall/membrane/envelope biogenesis (4.45 %) or extracellular structures and a number of significantly down-regulated genes responsible for defense mechanisms (6.02 %).

From the microarray data of 2, 4, and 8 wpi nodules, we first focus on the ferritin gene which had high expression at 8 wpi. Iron-containing proteins (ferritin) play a key role in crucial processes such as respiration, photosynthesis and DNA or hormone syntheses. During senescence, Protein degradation and membrane disruption followed oxidative stress lead to the significant increase of free iron concentration. The ferritin kept harmless from iron exceed in cells. Mostly cell wall of the nodules have many leghemoglobin that have iron-containing. At the senescence stage, the leghemoglobin decline associated with the low expression of leghemoglobin gene at 8 wpi (Figure 12a). This result was supported to the concentration of free iron from cell wall decreased (Figure 11a) in the nodules at 10 dai until 8 wpi.

The concentration of free iron from cell sap increased and then reduced in the nodule at 8 wpi (Figure 11b). The result suggested that a ferritin as iron-storage protein temporary accumulated at maturation stage of *L. japonicus* nodule because usually the plants remobilized nutrients together with metal ion, especially iron to shoot. Observation of the response to iron overload in cells by showing of high ferritin expression during nodule development (Figure 12b). When NO donor was applied with the nodules, expression of the ferritin increased (Figure 13a) while decreased when the nodule intact with NO scavenger (CPTIO). In the same way, the ferritin genes was high expression when treated with iron-citrate and was low expression when treated with iron scavenger (DFOM) in Figure 13b.

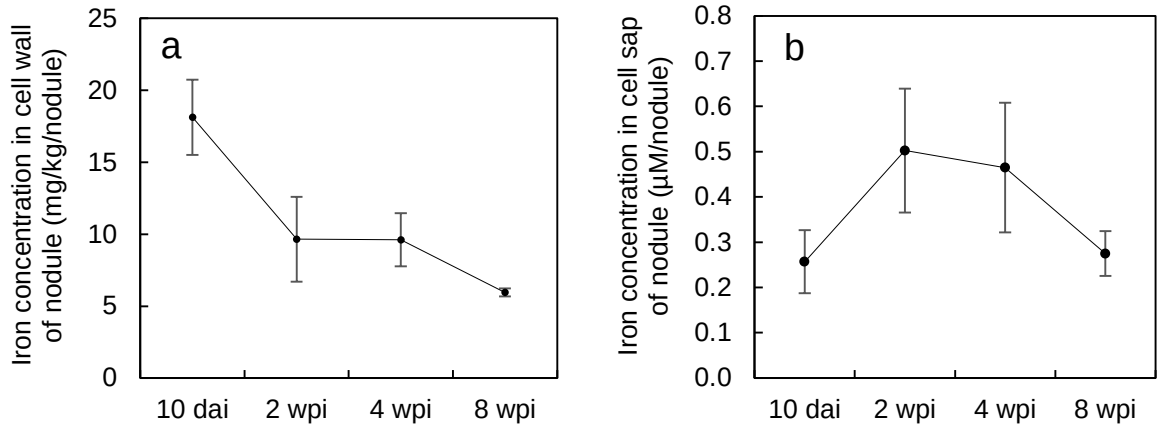

Figure 11 The concentration of free iron from cell wall (a) from cell sap (b) of *L. japonicus* nodules was shown detection by ICP-MS. Dai = day after inoculation, Wpi = weeks post inoculation

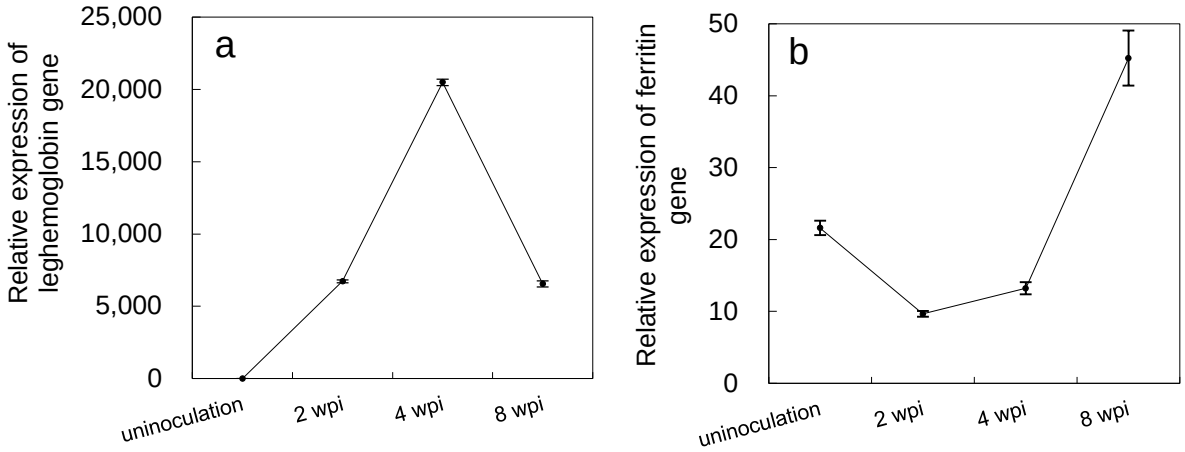

Figure 12 The expression pattern of leghemoglobin gene (a), and ferritin gene (b) expressed during nodule development analysis by qRT-PCR. Wpi = weeks post inoculation

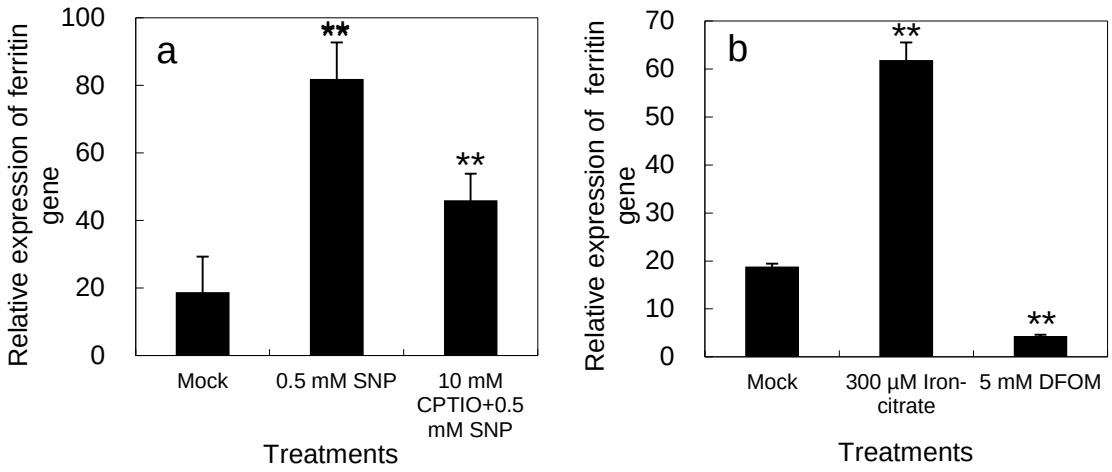

Figure 13 The expression pattern of ferritin expressed (a) when treated with sodium nitroprusside (SNP): NO donor and 2-4carboxyphenyl-4, 4, 5, 5-tetramethylimidazoline-1-oxyl-3-oxide (CPTIO): NO scavenger, and ferritin expression (b) was treated with iron-citrate (Fe (III)-citrate) and desferoxamine mesylate salt (DFOM): Fe scavenger, Mock is control treated with distrilled water (DW). The nodules at 4wpi were used. All data are shown ± SD. Statistically significant differences compared with mock are indicated with ** (P<0.01). Ubiquitin are reference gene.

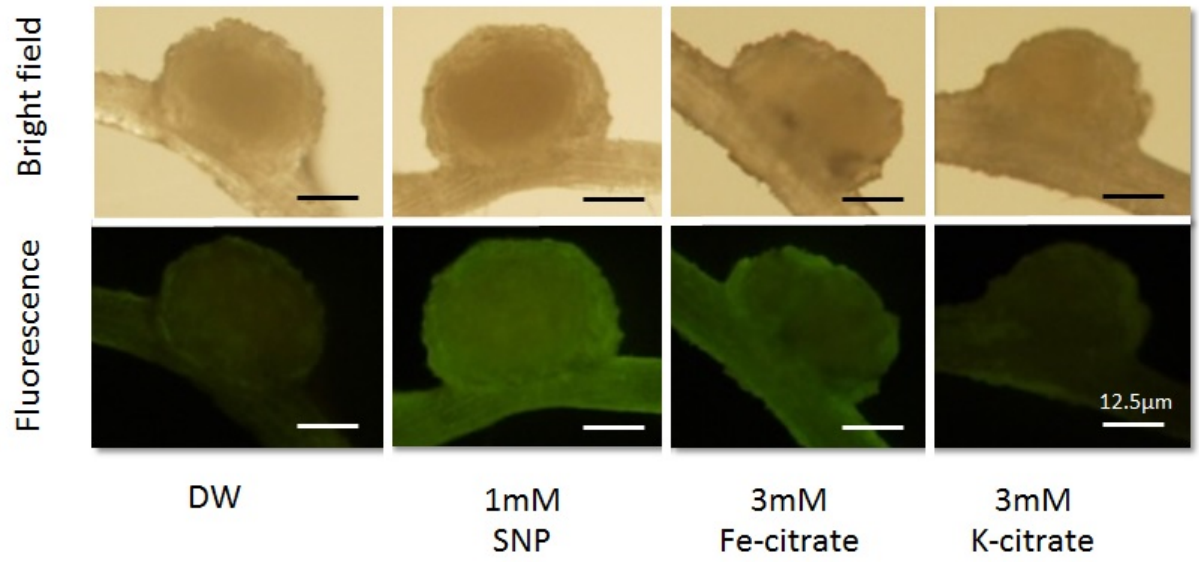

Figure 14 Nitric oxide was detected by DAF-FM when the nodules at 8 day after inoculation (dai) were treated with 1mM nitroprusside: NO donor, 3mM Fe-citrate and 3mM K-citrate, Distilled water (DW) is control, bar = 12.5µm.

The iron-dependent regulatory sequence (IDRS) was found in a promoter of ferritin gene in *L. japonicus*. The sequence CACGAGCTCGCCAC is position from -237 to -224 base pair. The strongly fluorescence was detected in the nodule that intact with SNP and iron-citrate treatments. Free iron stimulated NO signal in the nodules (Figure14) and the result in Figure 13 shows that nitric oxide as a signal to induce the ferritin expression. These data suggest that NO is required for iron-induced ferritin accumulation.

To summarize, we gained more knowledge about function of senescent process. GSI deficiency in bacteroid was likely motive early nodule senescence because metabolic compound decreased as well as nodule development changed. Many defense related genes were decreased in the senescent stage. Accumulation of iron in the cell sap of senescence nodule might induce the NO signal to express the ferritin. Ferritin accumulation might act homeostasis role at senescence stage. Metabolites will be translocated from senescing tissue to developing tissues in mature nodule for nutrition recycle. Additionally, basic data can be useful for the study of genes associated with accelerated or postponed senescence that is important for agriculture crop.